J. Fluid Mech. (1993), *vol.* 256, *pp.* 199–213
Copyright © 1993 Cambridge University Press

Monte Carlo simulation of the Taylor–Couette flow of a rarefied gas

By STEFAN STEFANOV[1] AND CARLO CERCIGNANI[2]

[1] Institute of Mechanics and Biomechanics, Bulgarian Academy of Sciences, Sophia, Bulgaria

[2] Dipartimento di Matematica, Politecnico di Milano, Milano, Italy

(Received 19 January 1993 and in revised form 14 May 1993)

We report and discuss the results of a direct Monte Carlo simulation of the flow of a rarefied gas flowing between two cylinders when the inner one rotates. The formation of Taylor vortices is clearly exhibited.

> The next great era of awakening of human intellect may well produce a method of understanding the qualitative content of equations. Today we cannot. Today we cannot see that the water flow equations contain such things as the barber pole structure of turbulence that one sees between rotating cylinders. (From *The Feynman Lectures on Physics.*)

1. Introduction

While the problems related to the instability of fluids and their transition to turbulence have been studied for a long time in classical hydrodynamics, the corresponding problems in kinetic theory have been paid attention only recently. This circumstance is clearly related to the extremely complex character of such problems when attacked with the Boltzmann equation. It is clear, however, that the study of such problems might be of greater importance for understanding fundamental phenomena of instability and self-organization in molecular dynamics. Encouraged by the positive result of our previous investigation (Stefanov & Cercignani 1992; Cercignani & Stefanov 1992) of Bénard's instability by means of the direct simulation Monte Carlo method (DSMC), recently we discussed (Stefanov & Cercignani 1993) the fluctuations of the macroscopic quantities in a rarefied gas flowing in a channel under the action of a constant external force in a direction parallel to the walls. Our final aim there was to study the transition to turbulence by means of the Boltzmann equation, but we remained far from achieving this goal, since our calculations were restricted to a two-dimensional geometry.

Here we report and discuss our computations concerning Taylor's instability of Couette flow, another well-known phenomenon in hydrodynamics. The classical case of this flow occurs when we consider two coaxial cylinders of infinite length and the inner cylinder rotates while the outer one is at rest. At a certain critical value of the angular velocity Ω of the rotating cylinder, the Couette flow becomes unstable and transforms into the so-called Taylor–Couette flow. This flow is characterized by a system of Taylor cells in the form of toroidal vortices, two neighbouring vortices rotating in opposite directions. A study of the same phenomenon in the framework of kinetic theory has never been attempted before. Our results refer to Knudsen numbers of order 10^{-2} and different Mach numbers, based on the velocity of the inner cylinder.

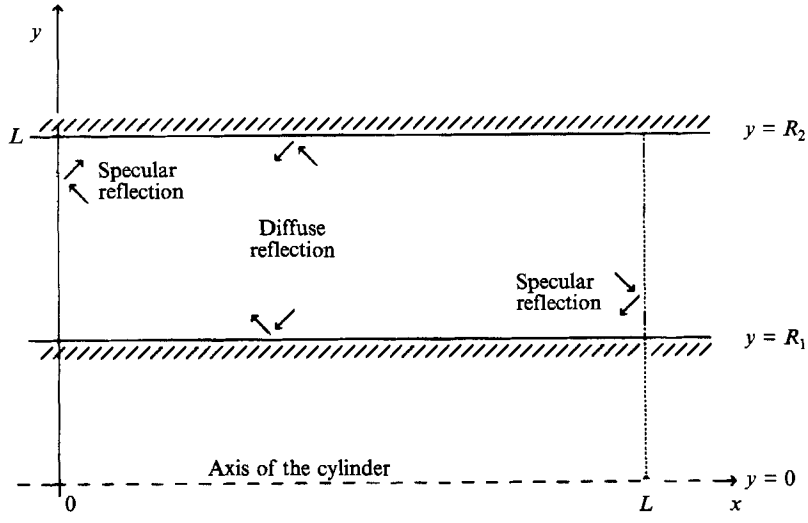

FIGURE 1. Geometry and boundary conditions.

The ranges of these numbers are chosen in such a way as to indicate the onset of instability in the cylindrical Couette flow of a rarefied gas. When the Taylor–Couette flow appears to be fully developed we extend our study to higher Mach numbers and exhibit results that seem to indicate transition to chaotic behaviour. Again the real physics of the transition to turbulence escapes these computations because of their two-dimensional nature.

Perhaps one might ask the question: Why solve the Boltzmann equation when $Kn = 10^{-2}$? Surely it would be sufficient to treat the problem as a perturbation about the Navier–Stokes equations. The answer is: well, we do not know. The Knudsen number mentioned here is either based on the radius of the inner cylinder or on the gap's width; but what is the Knudsen number to be taken into account in order to describe the rarefaction effects in the instability that leads to Taylor cells? From the results one sees that the Knudsen number based on the distance over which there is an important gradient in a cell is about one fifth of the gap's width and a factor 5 in the Knudsen number completely changes the order of magnitude of the perturbations, which can no longer be regarded as 'small'. The issues that appear in this connection are so many that only a study of comparable complexity for the Navier–Stokes equations (including compressibility at very large Mach numbers and slip effects) could give us an answer. A study that takes into account compressibility, but not slip, has been recently published (Hatay, Biringen & Zorumski 1993). The results of that paper seem to indicate that the critical Taylor number moves away from its classical value in the opposite direction to the results obtained here. This seems to indicate that the rarefaction effects play a very important role. It is thus clear that the present paper is not the last word on this subject. The authors only claim that they have broken some ground and will be quite happy if this paper suggests more advanced work on this problem.

Another issue that has stimulated the study presented here is the question, which is frequently raised, concerning the ability of the DSMC technique to faithfully resolve vortex motion, owing to the lack of accurate conservation of angular momentum in collisions. It seems that the first paper to cast doubts on this ability is Meiburg (1986), who applied both molecular dynamics and the direct simulation Monte Carlo method

to the case of a rarefied flow past an impulsively started inclined flat plate. A clear vortex structure was obtained in the wake region of the molecular dynamics calculation, but the wake in the direct simulation Monte Carlo method was relatively devoid of structure. As pointed out by Bird (1993), the approximations associated with either method cannot be tested for the unsteady flow past a plate because this problem places excessive demands on computer time. He therefore introduced the forced vortex flow produced by a moving wall in a two-dimensional cavity as an alternative test case and came to the conclusion that as long as the cell size requirement is met, the non-conservation of angular momentum in collisions does not appear to have a significant effect on the results of direct simulation Monte Carlo calculations. Bird (1993) also examined the values of the parameters in Meiburg's (1986) calculations and showed that the density of the gas was too high to employ the direct simulation Monte Carlo method, because the mean free path was of the order of the molecular diameter and the size of the cell is too large to analyse the vortical wake structure. The issue of non-conservation of angular momentum was addressed by Nanbu, Watanabe & Igarashi (1988), who showed that if the cell is sufficiently small, the total angular momentum of the molecules in a cell is almost conserved in the Monte Carlo calculations.

2. Basic equations

Let us consider a monatomic rarefied gas with average number density n_0 in unsteady motion between two coaxial cylinders with equal temperatures T_w, located at $r = R_1$ and $r = R_2$, respectively (see figure 1, which represents the section of half the cylinder in the x, y-plane). The inner cylinder rotates with angular velocity Ω, while the outer one is at rest. The Boltzmann equation reads as follows (Cercignani 1988, 1990; Kogan 1969):

$$\frac{\partial f}{\partial t}+\xi_1\frac{\partial f}{\partial x}+\xi_2\frac{\partial f}{\partial y}+\xi_3\frac{\partial f}{\partial z}=Q(f,f), \tag{2.1}$$

where $\boldsymbol{x}=(x,y,z)$ and $\boldsymbol{\xi}=(\xi_1,\xi_2,\xi_3)$ are the position and velocity vectors of a molecule, while

$$Q(f,f)=\frac{1}{m}\int\!\!\int(f'f'_*-ff_*-ff_*)\,B(\theta,|\boldsymbol{\xi}-\boldsymbol{\xi}_*|)\,\mathrm{d}\boldsymbol{\xi}_*\,\mathrm{d}\theta\,\mathrm{d}\epsilon \tag{2.2}$$

is the collision operator. Here $B(\theta,|\boldsymbol{\xi}-\boldsymbol{\xi}_*|)$ is a kernel describing the details of molecular interaction, m is the molecular mass, f', f'_*, f_* are the same as f, except that $\boldsymbol{\xi}$ is replaced by $\boldsymbol{\xi}', \boldsymbol{\xi}'_*, \boldsymbol{\xi}_*$. Also, $\boldsymbol{\xi}_*$ is an integration variable (the velocity of any molecule colliding with a molecule of velocity $\boldsymbol{\xi}$) while $\boldsymbol{\xi}'$ and $\boldsymbol{\xi}'_*$ are the velocities of two molecules entering a collision which brings them to velocities $\boldsymbol{\xi}$ and $\boldsymbol{\xi}_*$. Finally, θ and ϵ give the direction along which these molecules approach each other. We shall assume hard-sphere molecules, in which case $B(\theta,|\boldsymbol{\xi}-\boldsymbol{\xi}_*|)=\sigma^2|\boldsymbol{\xi}-\boldsymbol{\xi}_*|\cos\theta\sin\theta$, where σ is the sphere diameter.

We should rewrite the Boltzmann equation in cylindrical coordinates (x, r, ϕ), since we are looking for solutions independent of ϕ. We shall not do this here, since we take advantage of the cylindrical symmetry by exploiting a method described by Bird (1989*a*) (see the next section).

The non-dimensional parameters here are the Knudsen number Kn_L based on the thickness of the gap $L = R_2 - R_1$ ($Kn_L = \lambda_0/L$), the speed ratio $S = \Omega R_1/V_{th}$ (where $V_{th} = (2RT_w)^{\frac{1}{2}}$ is the thermal speed) related to the Mach number Ma by

$$Ma = (\tfrac{6}{5})^{\frac{1}{2}}S = 1.095\,S,$$

and the Knudsen number Kn_1 based on the inner cylinder radius R_1 ($Kn_1 = \lambda_0/R_1$). The basic parameter governing stability should be the Taylor number:

$$T = \frac{4\Omega^2 R_1^4}{\nu^2[1-(R_1/R_2)^2]^2} = \left(\frac{16}{5}\right)^2 4S^2\pi^{-1}\left(\frac{R_1}{\lambda_0}\right)^2 L^{-2}(L+R_1)^4(2L+R_1)^{-2}$$

$$= (13.04)S^2(Kn_1)^{-2}\left(1+\frac{Kn_L}{Kn_1}\right)^4\left(2+\frac{Kn_L}{Kn_1}\right)^{-2}, \quad (2.3)$$

where we have used the fact that ν is given by

$$\nu = (5/16)\lambda_0 V_{th}\pi^{\frac{1}{2}} \quad (2.4)$$

according to the Chapman–Enskog first approximation (Chapman & Cowling 1952), which is sufficiently good for our purposes.

If we are close to the continuum regime, we can then conjecture that the Taylor number remains the basic parameter to investigate stability. In the case of $Kn_L = Kn_1$ (i.e. when outer radius is twice the inner radius), the critical value of the Taylor number, according to the Navier–Stokes equations (with no slip) is 33110 (Chandrasekhar 1961, p. 323).

We complete our formulation with the following initial and boundary conditions:

(*a*) at time zero we assume equilibrium with the outer cylinder

$$f(0,x,y,\xi) = n_0\pi^{-\frac{3}{2}}V_{th}^{-3}\exp(-\xi^2/V_{th}^2); \quad (2.5)$$

(*b*) at the cylinders we assume diffuse reflection of the molecules and hence write

$$f(t,x,R_1,\xi) = n_1\pi^{-\frac{3}{2}}V_{th}^{-3}\exp(-|\xi-\Omega R_1 i|^2/V_{th}^2) \quad (\xi_2 \geqslant 0), \quad (2.6)$$

$$f(t,x,R_2,\xi) = n_2\pi^{-\frac{3}{2}}V_{th}^{-3}\exp(-\xi^2/V_{th}^2) \quad (\xi_2 \leqslant 0), \quad (2.7)$$

where i is the unit vector along the x-axis (which is also the cylinder axis), while n_1 and n_2 are determined by mass conservation at the walls and hence are given by

$$\left.\begin{aligned} n_1 &= (2\pi^{\frac{1}{2}}/V_{th})\int_{\xi_2>0} f(x,R_1,\xi)\,\xi_2\,\mathrm{d}^3\xi, \\ n_2 &= (2\pi^{\frac{1}{2}}/V_{th})\int_{\xi_2<0} f(x,R_2,\xi)\,\xi_2\,\mathrm{d}^3\xi; \end{aligned}\right\} \quad (2.8)$$

(*c*) in order to solve the problem numerically we assume that the solution possesses a periodic structure in the direction of the x-axis. We denote by $2\hat{L}$ the period in the x-direction and, in order to reduce the size of the sample, we simply assume specular reflection at $x = 0$ and $x = \hat{L}$.

3. Method of solution

The main idea on how to simulate rarefied gas flows with cylindrical symmetry is explained by Bird (1989*a*). At the start of each of the time steps Δt through which the molecules are moved, all the molecules are assumed to have the same value of z (because we want to treat y as a radial coordinate) and only coordinates x_i and y_i need be stored for the ith molecule, together with the three velocity components ξ_{ik}

($k = 1, 2, 3$). The molecules are moved according to their velocity and acquire certain coordinates x_i^*, y_i^*, z_i^*; then the new abscissa is taken to be $x_i^+ = x_i^*$, while the new ordinate (actually a radial coordinate) is $y_i^+ = [(y_i^*)^2 + (z_i^*)^2]^{\frac{1}{2}}$. The new velocity components are computed by taking the components of the previous velocity in the x-direction and in the two directions parallel and orthogonal to the vector with components x_i^*, y_i^*.

The Monte Carlo simulation was devised in agreement with the formulation of §2 and the above remarks. The basic steps of the simulation are as follows:

(*a*) the time interval $[0, T]$, over which the solution was sought, was subdivided into subintervals with step Δt;

(*b*) the space domain was subdivided into cells with sides $\Delta x, \Delta y$;

(*c*) the gas molecules were simulated in the gap G with a stochastic system of N points having positions $x_i(t)$, $y_i(t)$ and velocities $\xi_i(t)$;

(*d*) at each time there are N_m molecules in the mth cell; this number is varied by computing its evolution in the following two stages:

Stage 1. The binary collisions in each cell are calculated without moving the particles.

Stage 2. The particles are moved, with the new initial velocities acquired after collision, in a local coordinate system in which y plays the role of radial coordinate (no collisions in this stage).

(*e*) Stages 1 and 2 are repeated until $t = T$.

(*f*) The important moments of the distribution functions are calculated by time averaging after a regime situation has been reached.

Let us now describe the two stages of the calculation mentioned in (*d*) in some detail. In Stage 1 we use Bird's (1989*a*) 'no time counter' scheme, which envisages the following two steps:

Step 1. Computation of the maximum number of binary collisions. Here we replaced Bird's formula

$$N_{cmax} = \tfrac{1}{2} N_m \langle n \rangle \langle \pi \sigma^2 |\xi_i - \xi_j| \rangle_{max} \Delta t \tag{3.1}$$

(where $\langle n \rangle$ is the average density in the cell) with

$$N_{cmax} = \frac{N_m (N_m - 1)}{2 V_{cell}} \langle \pi \sigma^2 |\xi_i - \xi_j| \rangle_{max} \Delta t, \tag{3.2}$$

where $V_{cell} = \pi \Delta x \Delta(r^2)$ is the cell volume, if we take into account the fact that we are working in cylindrical geometry. Equation (3.2) was proposed by Yanitsky (1991). The reason for this replacement is the fact that the number of particles in each cell varies in time according to Poisson statistics. Hence $N_m(N_m - 1)$ has an average equal to the square of the average of N_m and is thus more appropriate than $N_m \langle n \rangle V_{cell}$ in the estimate of the number of collisions when the flow is unsteady, given the fact that $\langle n \rangle$ has a large variance because we have a very small sample size in a cell (Koura 1990).

Step 2. N_{cmax} pairs (i,j) of particles are randomly chosen. Each of these pairs is 'collided' with probability $|\xi_i - \xi_j| / \langle |\xi_i - \xi_j| \rangle_{max}$. If the collisional event occurs, the velocities after collisions are calculated in the following way:

$$\xi_i^+ = \tfrac{1}{2}(\xi_i + \xi_j + \boldsymbol{k} |\xi_i - \xi_j|), \tag{3.3}$$

$$\xi_j^+ = \tfrac{1}{2}(\xi_i + \xi_j - \boldsymbol{k} |\xi_i - \xi_j|), \tag{3.4}$$

where $\boldsymbol{k}$ is a vector randomly distributed on the unit sphere. Otherwise the velocities are left unchanged.

Kn_L	Kn_1	S	Stable	T	Re
0.05	0.02	2	Yes	966328	180.54
0.02	0.02	1	Yes	57955	90.27
0.02	0.02	1.5	No*	130400	135.41
0.02	0.02	2	No	231822	180.54
0.02	0.02	3	No	521600	270.81
0.02	0.02	6	No	2086400	541.62
0.02	0.02	8	No	3709155	722.16
0.02	0.02	10	No	5795555	902.70
0.02	0.02	12	No^c	8345599	1083.24
0.02	0.02	15	No^c	13034000	1354.05
0.02	0.01	2	No	2640600	362.08
0.02	0.005	2	No*	14836207	722.16
0.01	0.02	2	No	105624	180.54

TABLE 1. Stability of cylindrical Couette flow (No^c means transition to chaos and No* indicates no clear tendency to form a stable vortex). T denotes the Taylor number and Re the Reynolds number.

In Stage 2 the new positions and velocities of the molecules are computed through the equations:

$$\left.\begin{aligned} x_i^+ &= x_i + \xi_{1i}\,\Delta t, \\ y_i^+ &= [(y_i + \xi_{2i}\,\Delta t)^2 + (\xi_{3i}\,\Delta t)^2]^{\frac{1}{2}}, \\ \xi_{1i}^+ &= \xi_{1i}, \\ \xi_{2i}^+ &= [\xi_{2i}(y_i + \xi_{2i}\,\Delta t) + \xi_{3i}^2\,\Delta t]/y_i^+, \\ \xi_{3i}^+ &= [\xi_{3i}(y_i + \xi_{2i}\,\Delta t) - \xi_{2i}\,\xi_{3i}\,\Delta t]/y_i^+. \end{aligned}\right\} \tag{3.5}$$

The particles with $y_i^+ \leqslant R_1$ or $y_i^+ \geqslant R_2$ are diffusely reflected according to (2.6)–(2.8); the particles with $x_i^+ \leqslant 0$ and $x_i^+ \geqslant L$ are re-injected at $-x_i^+$ or $2\hat{L} - x_i^+$ with specularly reflected velocities.

4. Results and discussion

The results of our calculations are summarized in table 1, where the cases marked 'No' correspond to the formation of Taylor vortices, while 'No^c' indicates that even the Taylor cells are not stable and one witnesses the transition to a chaotic motion. In the cases indicated 'No*' there are small vortices with no clear tendency to form a stable Taylor vortex. Let us first discuss the results for $Kn_L = Kn_1 = 0.02$ (i.e. when the outer radius is twice the inner radius), since it covers the large majority of the cases that we have considered. In this case the critical value of the Taylor number, according to the Navier–Stokes equations (with no slip) is 33110 (Chandrasekhar 1961, p. 323). The results in table 1 seem to indicate a value higher than 57955; as in the case of Bénard's instability (Stefanov & Cercignani 1992; Cercignani & Stefanov 1992), rarefaction (with the associated phenomenon of slip at the boundary) seems to increase the critical value.

One should compare these results with those obtained by Hatay *et al.* (1993) for compressible Navier–Stokes equations at Mach numbers ranging from 0 to 3. It is surprising to note that, according to their results, the effect of mere compressibility, without rarefaction, is to shift the critical value of the Taylor number in the direction

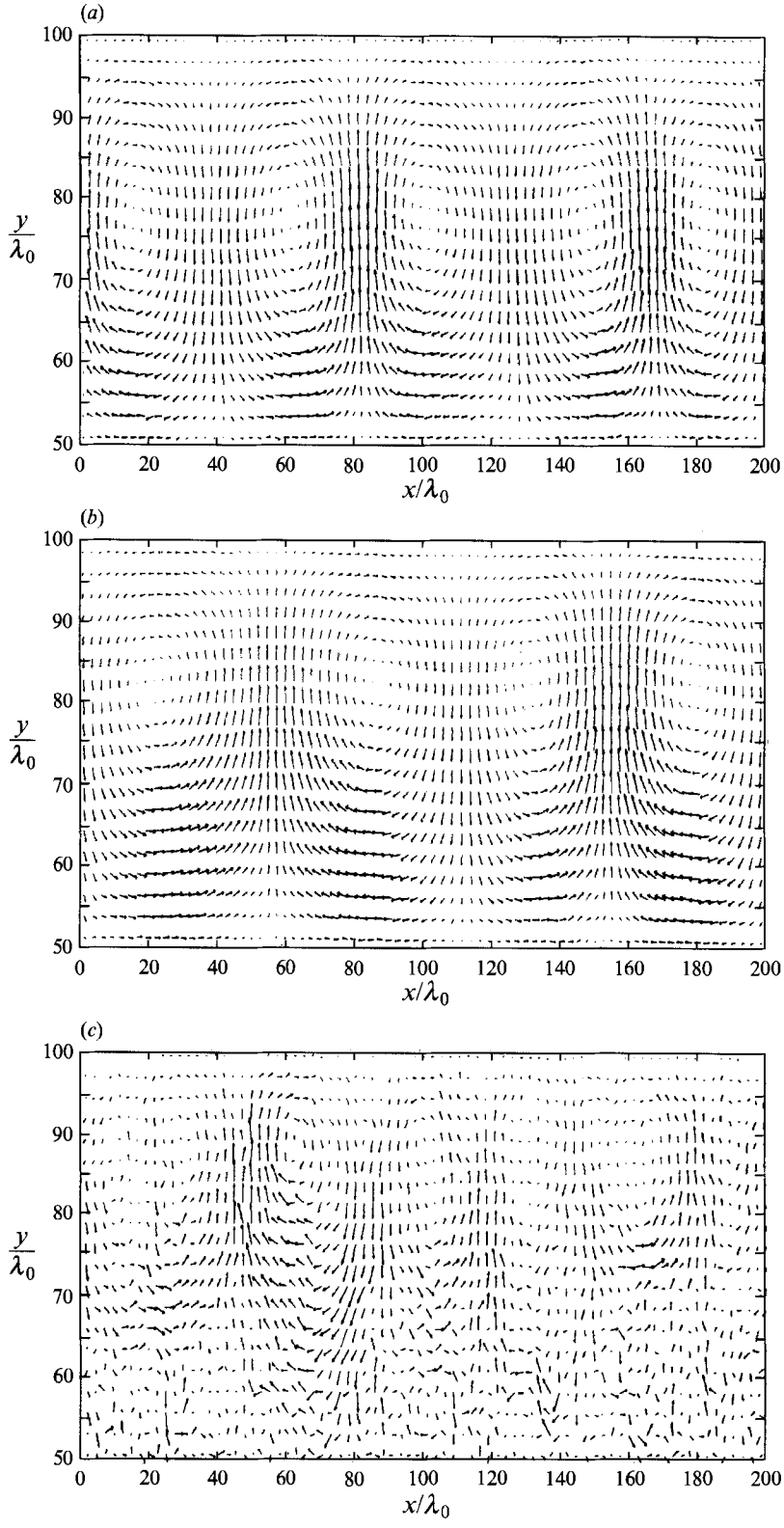

FIGURE 2. Velocity vector field for $Kn_L = Kn_1 = 0.02$, and (*a*) $S = 2$; (*b*) $S = 6$; (*c*) $S = 10$.

opposite to the one that we find with our kinetic theory calculations. Actually, in their paper the Reynolds number $Re = \Omega R_1^2/\nu$ based on the speed of the inner cylinder is used in place of the Taylor number. For this reason, this Reynolds number is also shown in table 1. Thus the disagreement with the Navier–Stokes equations seems to be higher than one would find by comparing with the classical result for the incompressible case. In fact, while a superficial estimate would indicate that the perturbation due to rarefaction would lead to a correction of, say, 2% in the critical Reynolds number and of 4% in the Taylor number, the real issue is what is the length to be used in the evaluation of the Knudsen number. If, as mentioned in the introduction, one takes the length over which there is a significant change of velocity in a vortex, this appears to be of the order of magnitude of one-fifth of the gap width and the above corrections should be multiplied by 5, and we would have found a satisfactory explanation of the numerical results, starting from the classical result holding for incompressible fluids. The role of compressibility is less clear and, according to Hatay *et al.*, seems to be larger than expected. We remark that their results were not obtained by solving the nonlinear Navier–Stokes equations, but rather a linearized version of them about the steady axisymmetric solution. The entire question of the role of compressibility seems worth a more detailed study in the future.

The other cases correspond to values of the parameter $\eta = Kn_L/(Kn_L + Kn_1)$ of $\frac{5}{7}$, $\frac{2}{3}$, $\frac{4}{5}$, $\frac{1}{3}$; thus strictly speaking we cannot consider 33110 as the critical value of the Taylor number according to the Navier–Stokes equations. The fact that for $Kn_L = 0.02$ and $Kn_1 = 0.005$ there is no clear tendency to form a stable vortex is perhaps, however, to be thought of as an indication of a transition to a chaotic motion. This type of dynamics is more clearly exhibited for higher values of the Taylor number.

We should also mention that our results refer to a choice of the thickness $\hat{L}$ equal to $4L$. We did some calculations with $\hat{L} = L$ and $\hat{L} = 2L$ which showed a not too strong dependence of the results upon the ratio $\hat{L}/L$. In any of these cases the vortex size was between $\frac{1}{2}L$ and L. The distance $\hat{L}$ was chosen to be large enough to obtain a set of vortices and was otherwise limited by problems related to computer memory and computation time.

The phenomena that we examine show up in flows with relatively small Knudsen numbers. The DSMC method requires the cell size to be less than or, at the very least, of the same order of magnitude as the mean free path. If we take into account these two requirements, we should carry out our calculations with a large number of particles and a grid with a large number of cells. These considerations led us to consider a rectangular domain of $400 \times 100 = 4 \times 10^4$ cells with an average number of particles per cell equal to 5 or 10. This means that we must consider from 2×10^5 to 4×10^5 molecules.

The final results to be presented here are obtained with an additional averaging over groups of cells (5×5) and thus refer to a mesh 80×20. For the purpose of commenting we subdivide the figures into four groups.

(*a*) Group I

In figures 2(*a*)–2(*c*) we present the velocity vector fields for some cases with $Kn_L = Kn_1 = 0.02$, indicated in table 1 above, for which the pure Couette flow is unstable. These are a pictorial illustration of the table and the discussion given above.

(*b*) Group II

The first five figures of this group (figures 3–7) show the isolines and three-

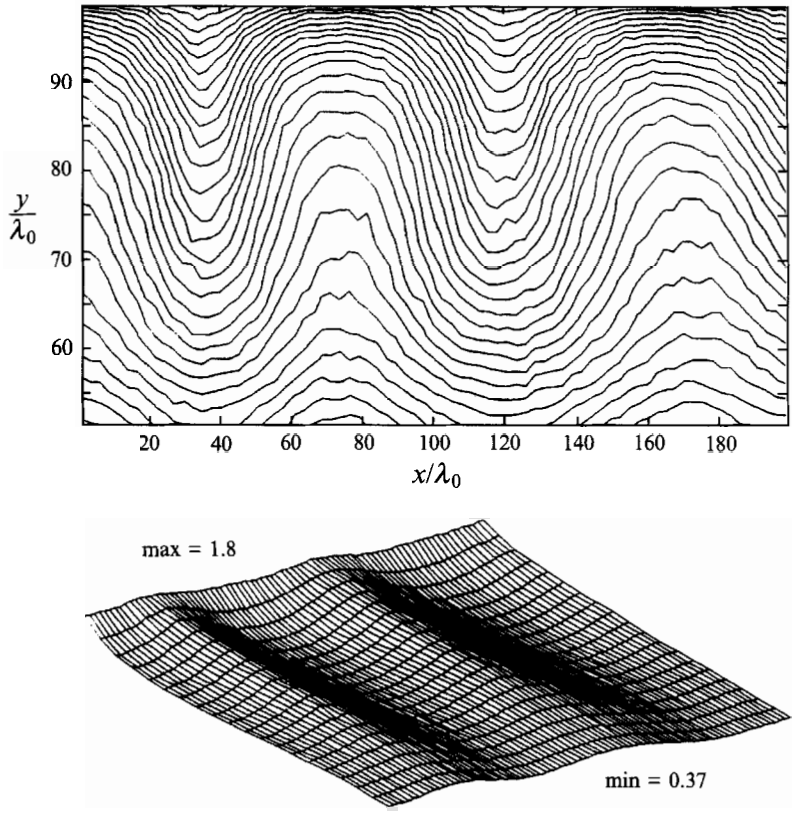

FIGURE 3. Isolines and three-dimensional plot of the number density $n(x, y)$ for $Kn_L = Kn_1 = 0.02$, $S = 3$.

dimensional plots of density, Mach number, velocity components in a typical case ($Kn_L = Kn_1 = 0.02$, $S = 3$). One sees that, while the first two quantities and the z-component of velocity seem to be more sensitive to the stratification induced by rotation than to the presence of vortices, the isolines of the velocity components in the (x, y) section of the cylinder create a vivid picture of what is going on when Taylor vortices are formed. Figure 8 shows the velocity contours in the case in which the Taylor vortices have disappeared and a chaotic motion is seen.

(*c*) Group III

In this group we could present a large number of pictures showing the behaviour of the energy spectral density as a function of the frequency. These pictures show that there is a largely dominating frequency for low values of the Taylor number, while other modes grow when the Taylor number increases. We refrain from presenting all the details and show only one picture (figure 9) which exhibits the energy spectral density of the dominating mode (in a logarithmic scale) as a function of the speed ratio S (for $Kn_L = Kn_1 = 0.02$). To be precise, we considered the fast Fourier transform $\widehat{v_x}$ of the x-component of velocity with respect to x for three values of y/λ (51.25, 56.25, 73.25). The largest values of $E = \frac{1}{2}|\widehat{v_x}|^2$ occurred at $y/\lambda = 56.25$ for all values of S. These largest values are plotted in figure 9 versus S; the maximum of the curve (here normalized to unity) occurs for $S = 6$; this means that in this case the Taylor cells form a very coherent and symmetrical structure well beyond any kind of fluctuation.

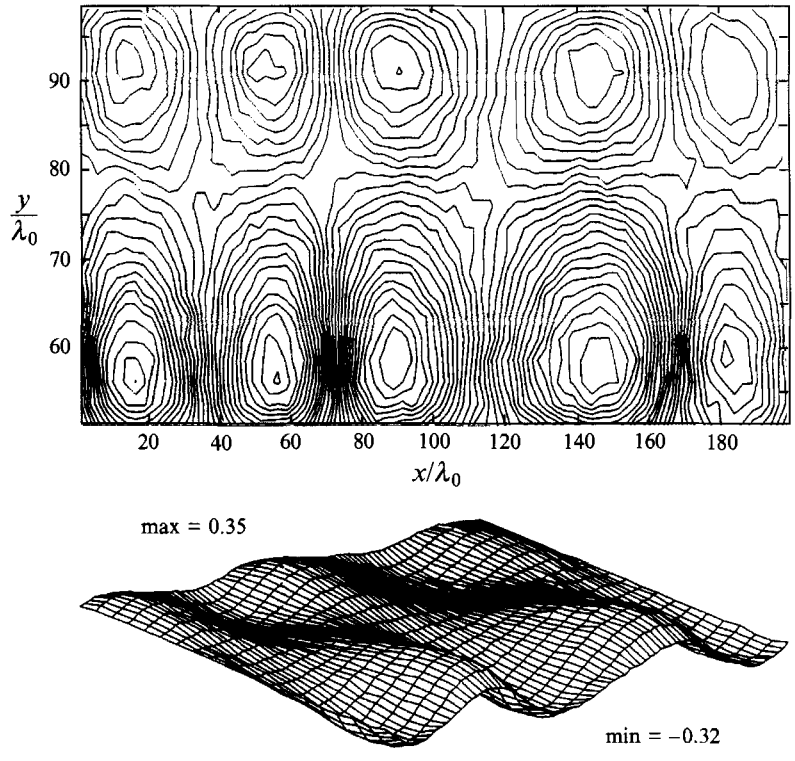

FIGURE 4. Isolines and three-dimensional plot of the x-component of velocity, $V_x(x, y)$ for $Kn_L = Kn_1 = 0.02$, $S = 3$.

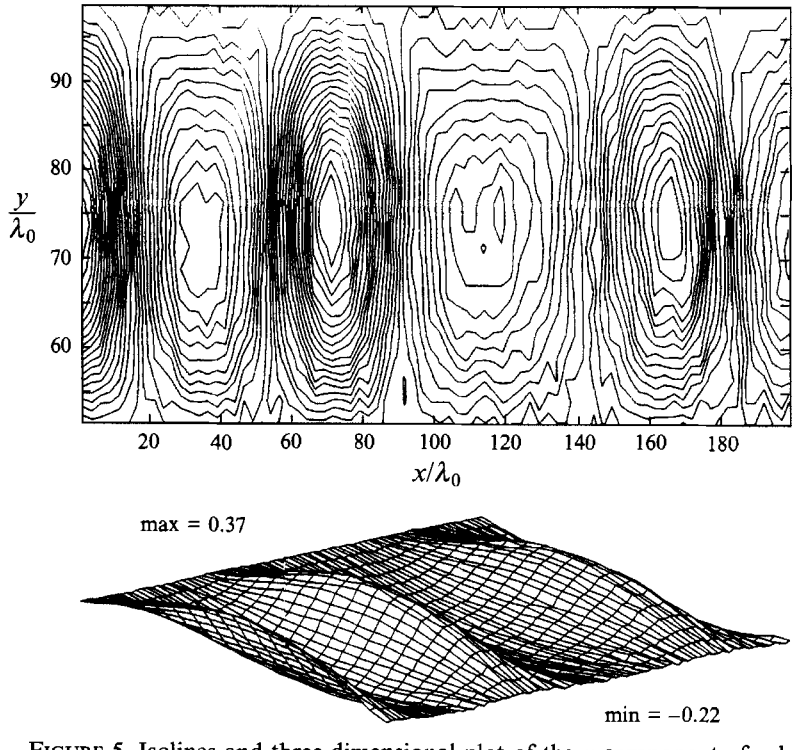

FIGURE 5. Isolines and three-dimensional plot of the y-component of velocity, $V_y(x, y)$ for the same case as figure 3.

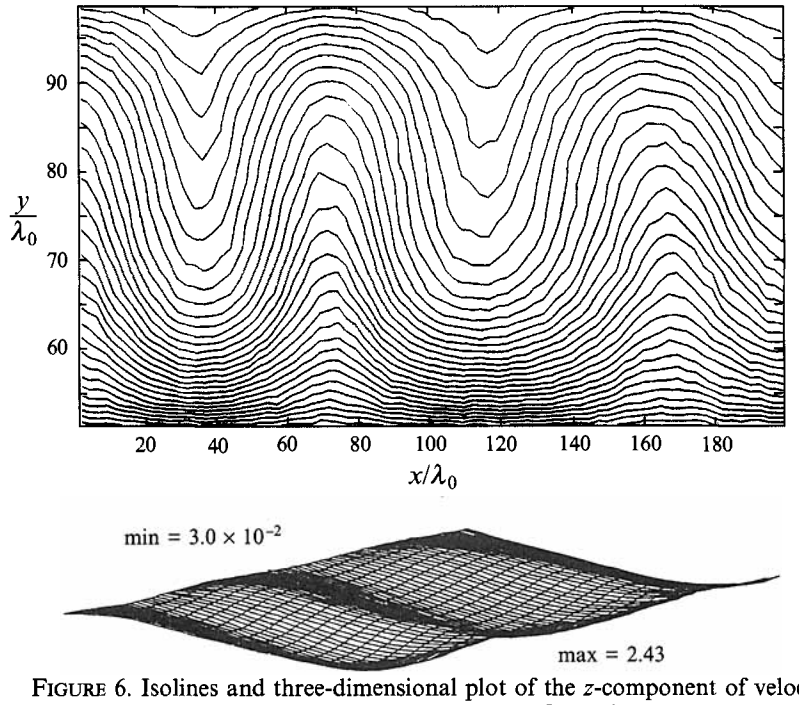

FIGURE 6. Isolines and three-dimensional plot of the z-component of velocity, $V_z(x, y)$ for the same case as figure 3.

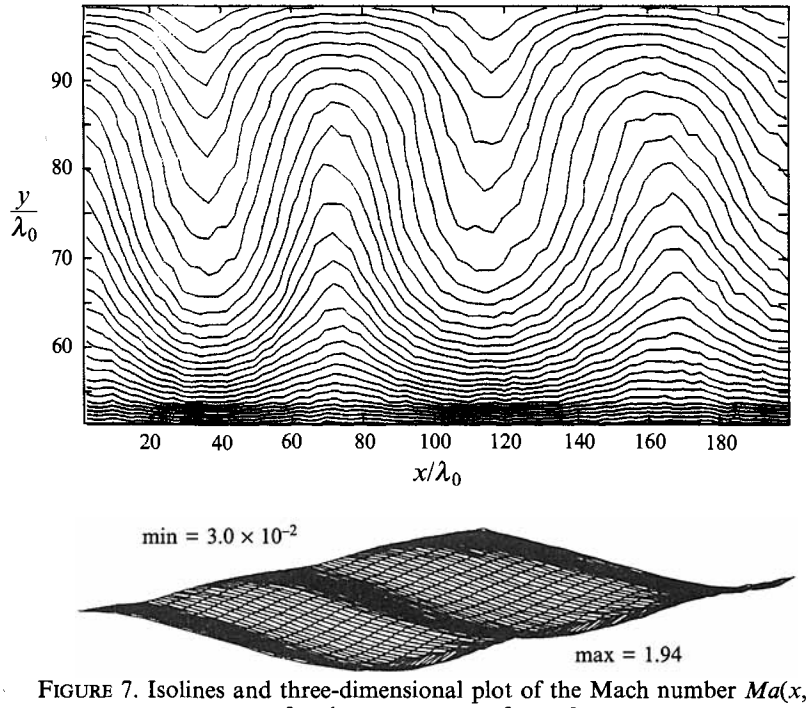

FIGURE 7. Isolines and three-dimensional plot of the Mach number $Ma(x, y)$ for the same case as figure 3.

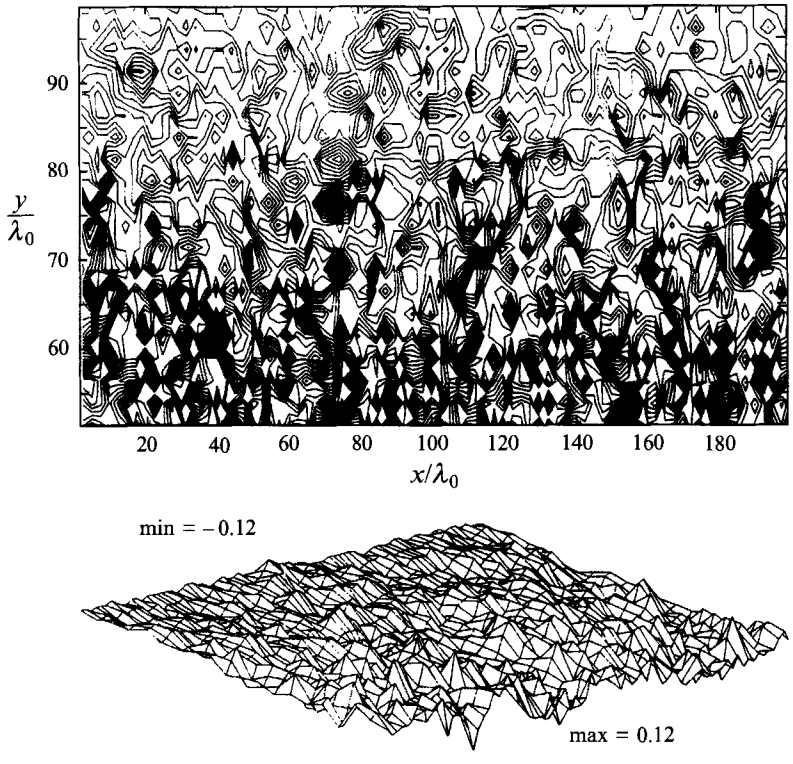

FIGURE 8. Isolines and three-dimensional plot of the x-component of velocity, $V_x(x, y)$ for $Kn_L = Kn_1 = 0.02$, $S = 15$.

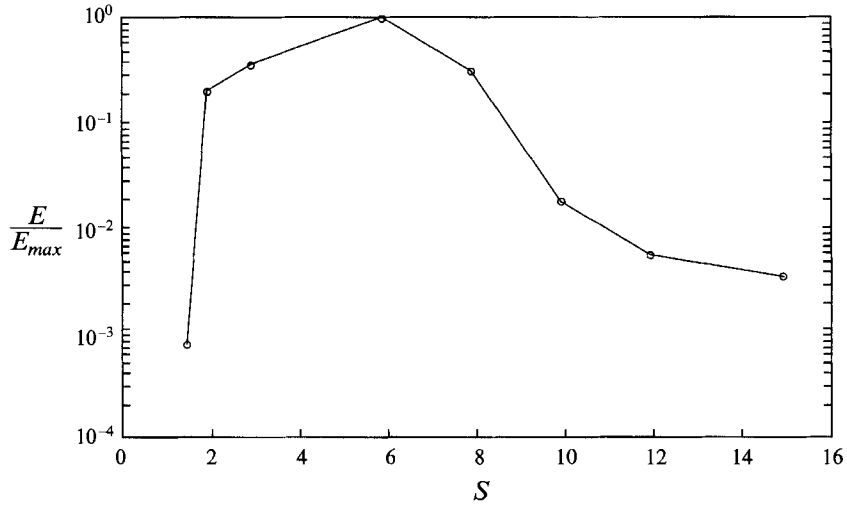

FIGURE 9. The energy spectral density of the dominating mode as a function of the speed ratio S (for $Kn_L = Kn_1 = 0.02$). The highest value is normalized to unity.

From the velocity field pictures, some of which are shown in Group I above, we see that at $S = 6$ we have a reduction of the number of cells in the gap from 5 to 4. After $S = 6$ the cells are less symmetrical and for $S = 8$ one begins to see some sign of

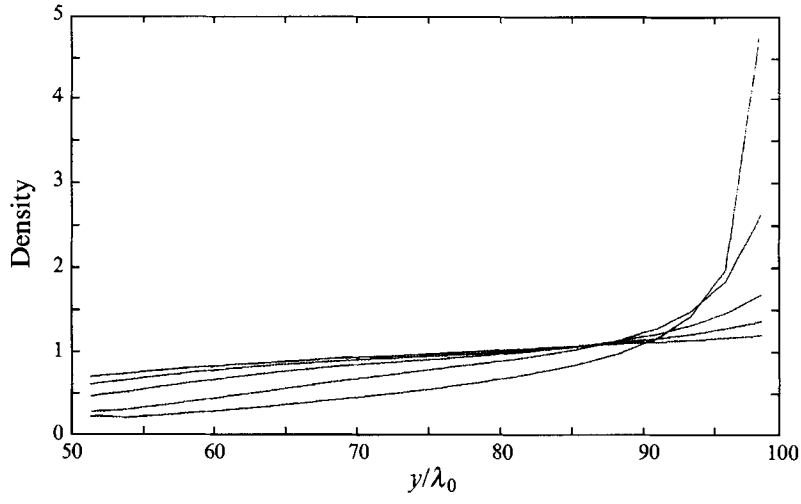

FIGURE 10. The mean profile of density for $Kn_L = Kn_1 = 0.02$; the average is taken with respect to x. The profiles refer to $S = 1.5$, $S = 2$, $S = 3$, $S = 6$, $S = 15$ (in this order downward at $y/\lambda = 50$).

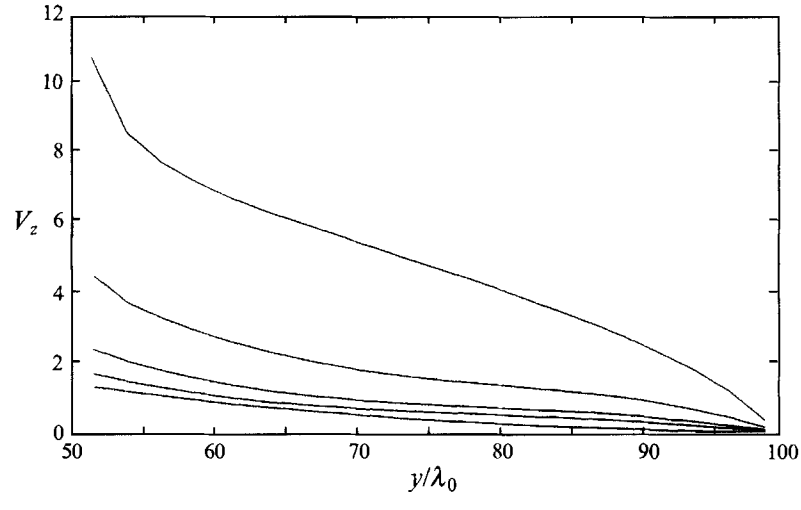

FIGURE 11. The mean profile of z-component of velocity for $Kn_L = Kn_1 = 0.02$; the average is taken with respect to x. The profiles refer to $S = 15$, $S = 6$, $S = 3$, $S = 2$, $S = 1.5$ (in this order downward at $y/\lambda = 50$).

instability; the power density of the dominating mode is reduced by a factor 50 with respect to the maximum and continues to decrease. When chaotic behaviour is established, some coherence is still present, because the energy of the dominating mode is about 250 times smaller than the highest value, but still 7 to 10 times larger than the statistical noise present in laminar flow. This clearly indicates that the chaotic behaviour shown by the calculations has nothing to do with the statistical noise of the Monte Carlo method.

(*d*) Group IV

These pictures (figures 10–13) are the mean profiles of density, z-component of velocity, Mach number and temperature for $Kn_L = Kn_1 = 0.02$; the average is taken

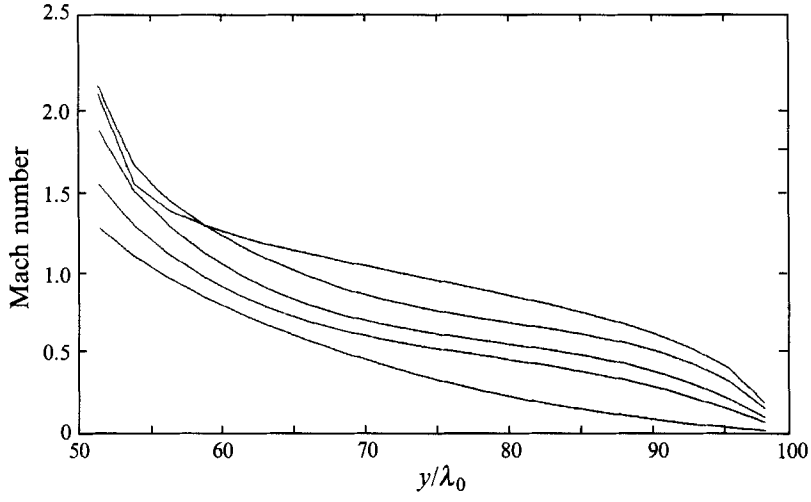

FIGURE 12. The mean profile of Mach number for $Kn_L = Kn_1 = 0.02$; the average is taken with respect to x, for the same S values as figure 11.

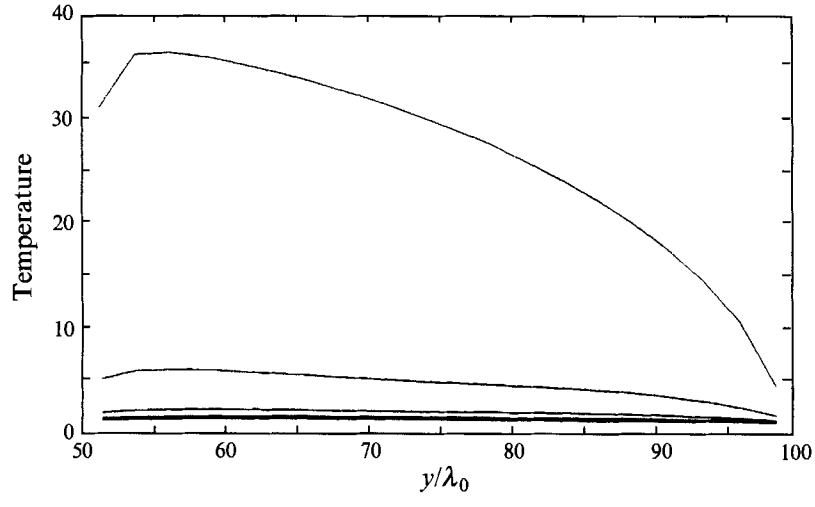

FIGURE 13. The mean profile of temperature for $Kn_L = Kn_1 = 0.02$; the average is taken with respect to x, for the same S values as figure 11.

with respect to x. An interesting feature is the change of curvature in the velocity and Mach number profiles. For $S = 1.5$, the profiles are convex everywhere, but for higher values of S, they show an inflexion point. It should be noticed that the profile of the Mach number for $S = 15$ crosses the profile corresponding to $S = 6$ rather close to the inner cylinder.

5. Concluding remarks

We have discussed the results arising from a numerical simulation of the behaviour of a monatomic rarefied gas in a flow between two cylinders, when the inner cylinder rotates. The gas clearly exhibits an instability for a Taylor number of the order of the

critical value for fluids governed by the Navier–Stokes equations; beyond that value, Taylor vortices appear. At another critical number a new instability occurs and a transition to chaotic dynamics is witnessed. A clear transition to turbulence cannot be completely uncovered, however, because our calculations are intrinsically two-dimensional.

This research was carried out when S.S. was visiting Politecnico di Milano with the financial support of the Gruppo Nazionale di Fisica Matematica of the Italian Research Council (CNR). The senior author (C.C.) gratefully acknowledges partial support of the latter agency and of Ministero per l'Università e la Ricerca Scientifica. S.S. also acknowledges the travel support obtained from the Bulgarian Government (Department of Education and Science, Grant N. MM46/91).

REFERENCES

BIRD, G. 1989*a* Comment on 'False collisions in the direct simulation Monte Carlo method' [Phys. Fluids 31, 2047 (1988)]. *Phys. Fluids* A **1**, 897.

BIRD, G. 1989*b* Perception of numerical methods in rarefied gas dynamics. In *Rarefied Gas Dynamics: Theoretical and Computational Techniques* (ed. E. P. Muntz, D. P. Weaver & D. H. Campbell), pp. 212–226. AIAA.

BIRD, G. A. 1993 Direct simulation of high-vorticity gas flows. *Phys. Fluids* **30**, 364–366.

CERCIGNANI, C. 1988 *The Boltzmann equation and its applications.* Springer.

CERCIGNANI, C. 1990 *Mathematical Methods in Kinetic Theory.* Plenum.

CERCIGNANI, C. & STEFANOV, S. 1992 Bénard's instability in kinetic theory. *Transport Theory Statist. Phys.* **21**, 371–381.

CHANDRASEKHAR, S. 1961 *Hydrodynamic and Hydromagnetic Stability.* Oxford University Press.

CHAPMAN, S. & COWLING, T. G. 1952 *The Mathematical Theory of Non-Uniform Gases.* Cambridge University Press.

HATAY, F. F., BIRINGEN, S. & ZORUMSKI, W. E. 1993 Stability of high speed compressible rotating Couette flow. *Phys. Fluids* A **5**, 393–404.

KOGAN, M. N. 1969 *Rarefied Gas Dynamics.* Plenum.

KOURA, K. 1990 A sensitive test for accuracy in evaluation of molecular collision number in the direct-simulation Monte Carlo Method. *Phys. Fluids* A **2**, 1287–1289.

MEIBURG, E. 1986 Comparison of the molecular dynamics method and the direct simulation Monte Carlo technique for flows around simple geometries. *Phys. Fluids* **29**, 3107–3113.

NANBU, K., WATANABE, Y. & IGARASHI, S. 1988 Conservation of angular momentum in the direct simulation Monte Carlo method. *J. Phys. Soc. Japan* **57**, 2877–2880.

STEFANOV, S. & CERCIGNANI, C. 1992 Monte Carlo simulation of Bénard's instability in a rarefied gas. *Eur. J. Mech.* B **5**, 543–552.

STEFANOV, S. & CERCIGNANI, C. 1993 Monte Carlo simulation of a channel flow of a rarefied gas. *Eur. J. Mech.* B (submitted).

YANITSKY, V. E. 1990 Operator approach to direct Monte Carlo simulation theory. In *Rarefied Gas Dynamics* (ed. A. Beylich), pp. 770–777. New York: VCH.